Supporting Information

Local Coordination Geometry Perturbed *β*-Diketone Dysprosium Single-Ion Magnets

*Jing Zhu, Changzheng Wang, Fang Luan, Tianqi Liu, Pengfei Yan, Guangming Li**

Key Laboratory of Functional Inorganic Material Chemistry (MOE); School of Chemistry and Materials Science, Heilongjiang University, Harbin 150080, P. R. China. E-mail: gmli_2000@163.com

Index

Scheme S1	Synthesis of complexes **1**–**3**.
Figure S1	IR spectra of the TFI and complexes **1**–**3**.
Figure S2	UV absorption spectra of the TFI and complexes **1**–**3**.
Figure S3-S5	TG-DSC curves of complexes **1**–**3**.
Figure S6-S8	The powder X-ray diffraction patterns and the simulated patterns of complexes **1**–**3**.
Figure S9	The π-π stacking and hydrogen bonds interactions between the molecules in complex **1**.
Figure S10	The hydrogen bonds interactions between the molecules in complex **2**.
Figure S11	The π-π stacking and hydrogen bonds interactions between the molecules in complex **3**.
Figure S12	M versus H / T plots at 1.8 K, 3.0 K and 5.0 K for complexes **1**–**3**.
Figure S13	Temperature dependence of ac susceptibility of complex **1** under 0 Oe in the frequency range 1–1000 Hz.
Figure S14	Temperature dependence of ac susceptibility of complexes **1**–**3** under 2000 Oe in the frequency range 1–1000 Hz.
Figure S15	Hysteresis loop for the complexes **2** and **3** at 1.8 K with the sweep rate at 50 Oe/s and 200 Oe/s.
Table S1	Selected bond length (Å) and angles (°) for complexes **1**–**3**.
Table S2	Fitted parameters of the Cole-Cole plots for complex **2** at H_{dc}= 0 G.
Table S3	Fitted parameters of the Cole-Cole plots for complex **3** at H_{dc}= 0 G.

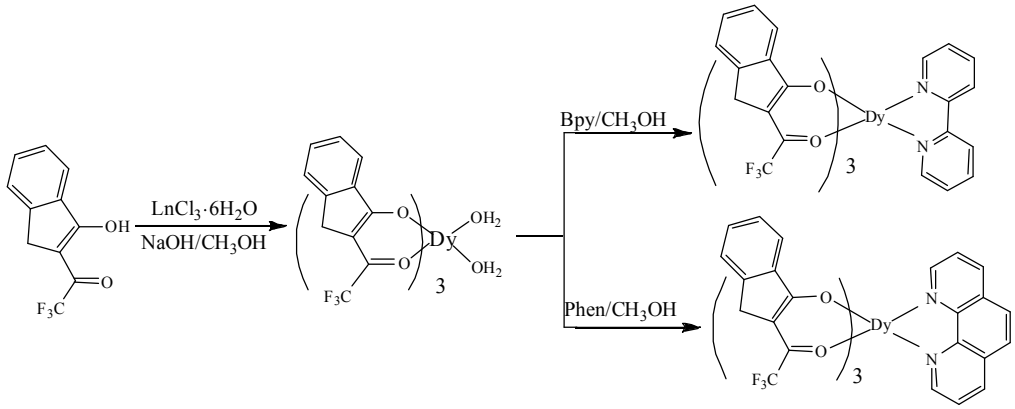

Scheme S1. Synthesis of complexes **1**–**3**.

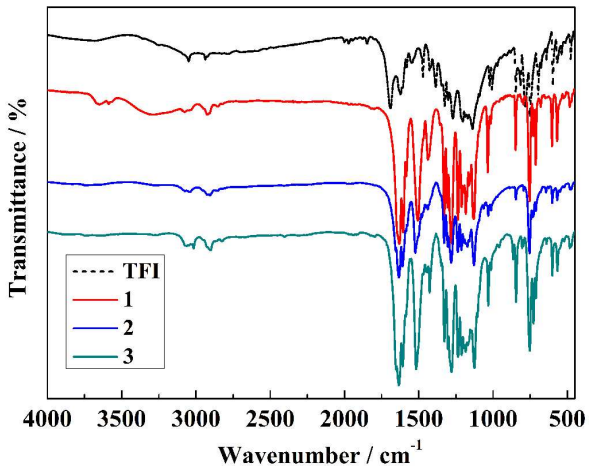

Figure S1. IR spectra of the TFI and complexes **1**–**3**.

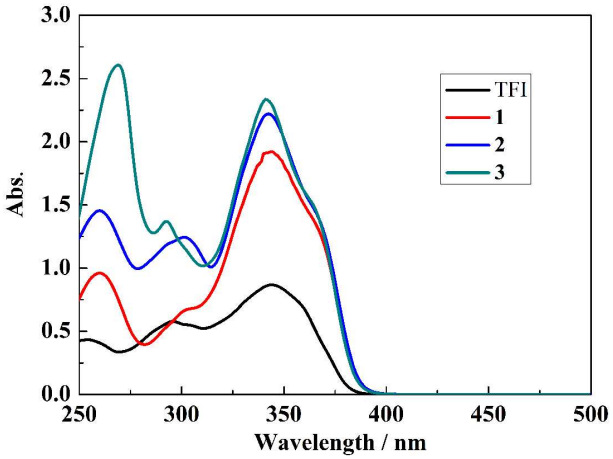

Figure S2. UV absorption spectra of the TFI and complexes **1**–**3**.

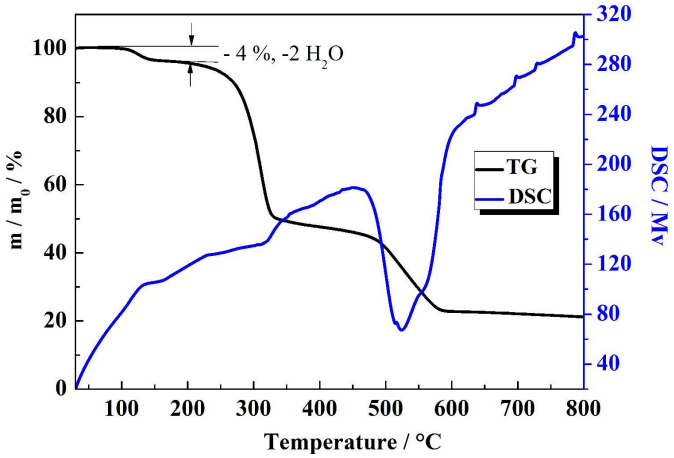

Figure S3. TG-DSC curves of complex **1**.

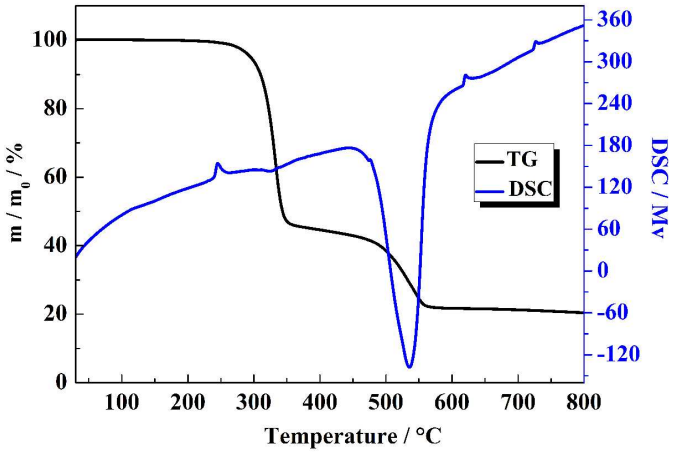

Figure S4. TG-DSC curves of complex **2**.

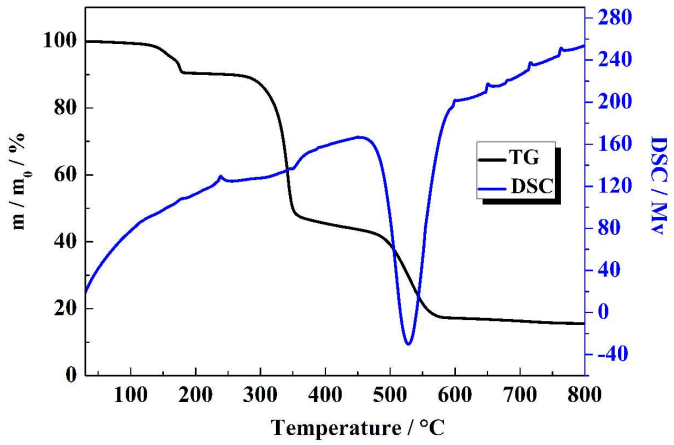

Figure S5. TG-DSC curves of complex **3**.

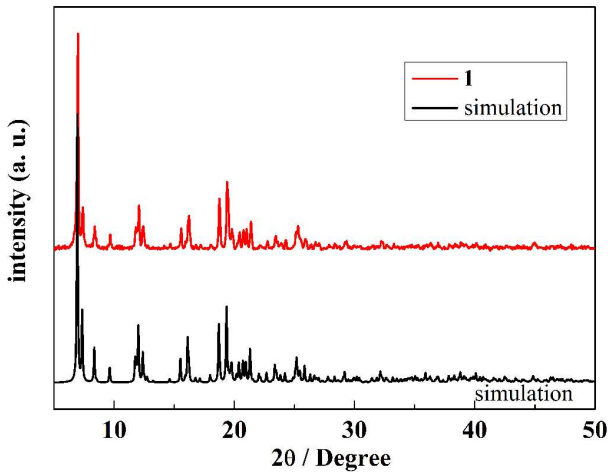

Figure S6. The powder X-ray diffraction patterns and the simulated patterns of complex **1**.

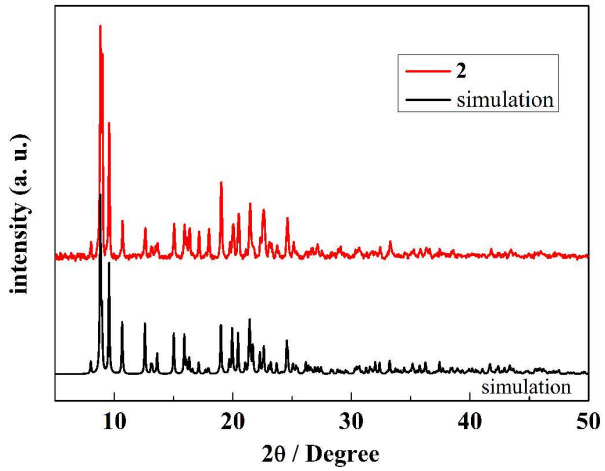

Figure S7. The powder X-ray diffraction patterns and the simulated patterns of complex **2**.

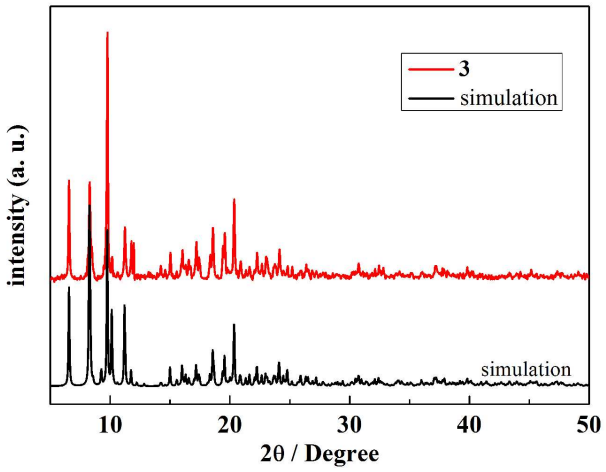

Figure S8. The powder X-ray diffraction patterns and the simulated patterns of complex **3**.

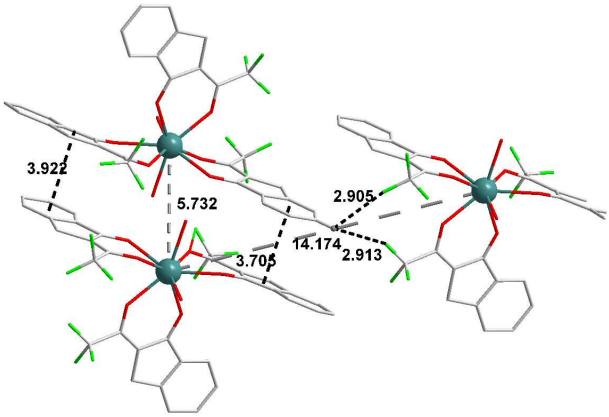

Figure S9. The π-π stacking and hydrogen bonds interactions between the molecules in complex **1** (Partial hydrogen atoms are omitted for clarity).

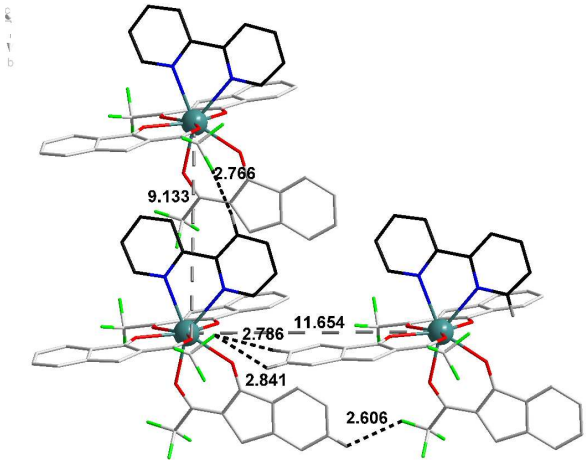

Figure S10. The hydrogen bonds interactions between the molecules in complex **2** (Partial hydrogen atoms are omitted for clarity).

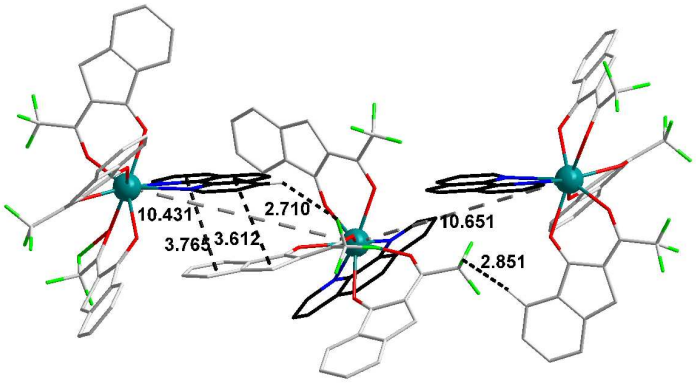

Figure S11. The π-π stacking and hydrogen bonds interactions between the molecules in complex **3** (Partial hydrogen atoms are omitted for clarity).

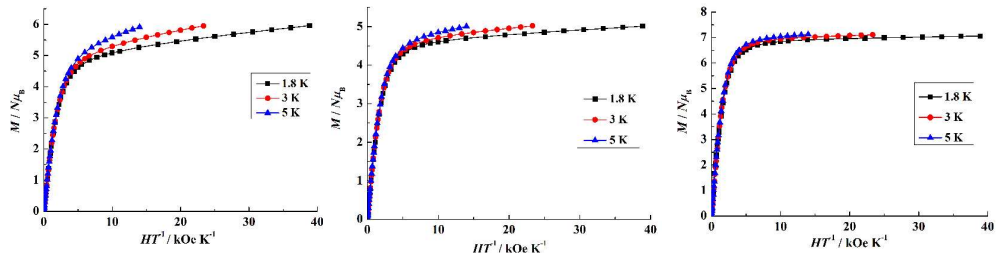

(a) (b) (c)

Figure S12. M versus H / T plots at 1.8 K, 3.0 K and 5.0 K for **1** (a), **2** (b) and **3** (c).

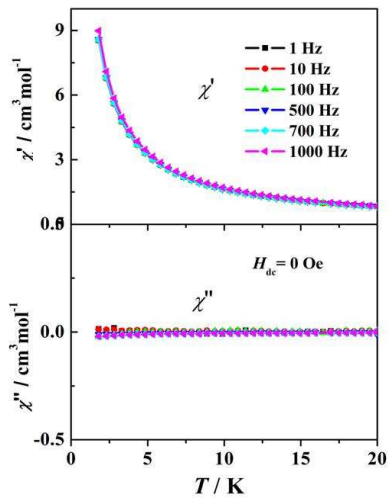

Figure S13. Temperature dependence of the in-phase (χ′) and out-of-phase (χ″) ac susceptibility of complex **1** under 0 Oe in the frequency range 1–1000 Hz.

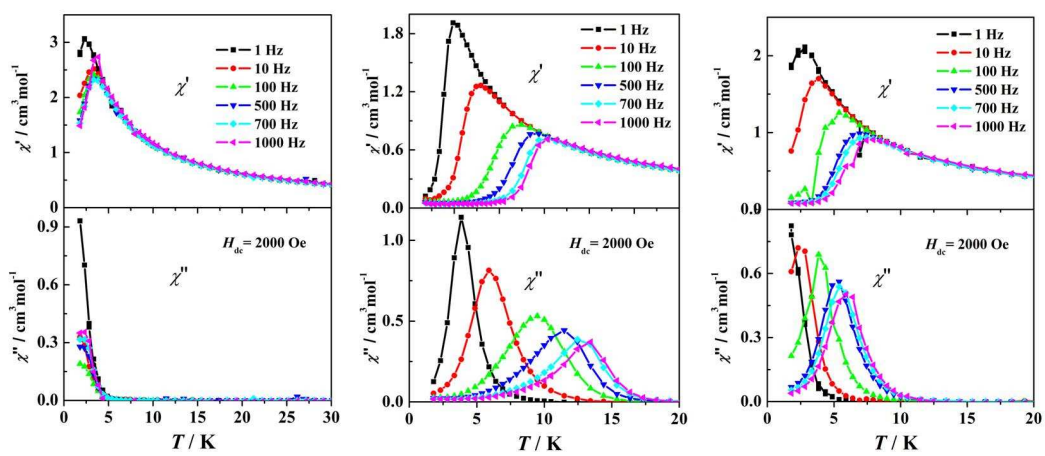

(a) (b) (c)

Figure S14. Temperature dependence of the in-phase (χ′) and out-of-phase (χ″) ac susceptibility of complexes **1** (a), **2** (b) and **3** (c) under 2000 Oe in the frequency range 1–1000 Hz in the temperature range of 1.8–20 K.

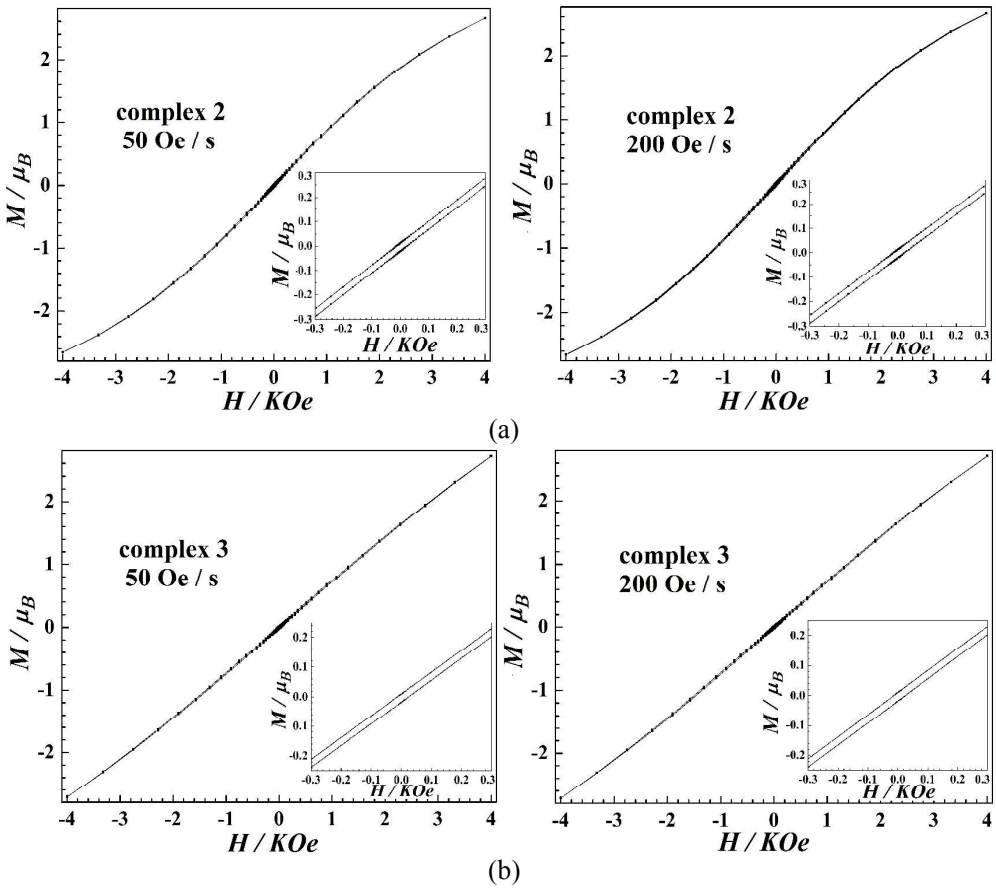

Figure S15. Hysteresis loop for the complexes **2** (a) and **3** (b) at 1.8 K with the sweep rate at 50 Oe/s and 200 Oe/s.

Table S1. Selected bond lengths (Å) and angles (°) for complexes **1**–**3**.

1			**2**	**3**
Dy(1)–O(1)	2.407(3)	Dy(1)–O(1)	2.315(6)	2.376(3)
Dy(1)–O(2)	2.332(3)	Dy(1)–O(2)	2.363(6)	2.315(3)
Dy(1)–O(3)	2.320(3)	Dy(1)–O(3)	2.328(6)	2.312(3)
Dy(1)–O(4)	2.314(4)	Dy(1)–O(4)	2.311(6)	2.347(3)
Dy(1)–O(5)	2.363(3)	Dy(1)–O(5)	2.359(6)	2.352(3)
Dy(1)–O(6)	2.364(3)	Dy(1)–O(6)	2.346(5)	2.312(3)
Dy(1)–O(7)	2.402(3)	Dy(1)–N(1)	2.566(7)	2.531(4)
Dy(1)–O(8)	2.418(3)	Dy(1)–N(2)	2.567(7)	2.532(4)
O(4)-Dy(1)-O(2)	123.48(13)	O(4)-Dy(1)-O(1)	92.6(2)	120.72(11)
O(3)-Dy(1)-O(2)	74.27(12)	O(1)-Dy(1)-O(3)	74.7(2)	73.09(11)
O(4)-Dy(1)-O(5)	77.64(12)	O(4)-Dy(1)-O(6)	148.3(2)	78.90(12)
O(3)-Dy(1)-O(5)	114.80(12)	O(1)-Dy(1)-O(6)	81.6(2)	140.54(12)
O(2)-Dy(1)-O(5)	76.69(10)	O(3)-Dy(1)-O(6)	75.2(2)	145.39(12)
O(4)-Dy(1)-O(6)	72.10(13)	O(4)-Dy(1)-O(5)	139.3(2)	75.33(11)
O(3)-Dy(1)-O(6)	140.22(12)	O(1)-Dy(1)-O(5)	102.3(2)	140.69(11)
O(2)-Dy(1)-O(6)	142.43(11)	O(3)-Dy(1)-O(5)	147.2(2)	79.14(12)
O(4)-Dy(1)-O(1)	137.58(11)	O(4)-Dy(1)-O(2)	76.0(2)	74.53(12)
O(3)-Dy(1)-O(1)	77.11(11)	O(3)-Dy(1)-O(2)	134.0(2)	109.66(12)
O(5)-Dy(1)-O(1)	143.24(11)	O(6)-Dy(1)-O(2)	130.4(2)	81.77(12)
O(6)-Dy(1)-O(1)	120.23(10)	O(5)-Dy(1)-O(2)	72.4(2)	144.30(11)

Table S2. Fitted parameters of the Cole-Cole plots for complex **2** at H_{dc}= 0 G.

T / K	χ_S	χ_T	a
1.8	0.45334	5.93758	0.12263
3.0	0.28735	3.65433	0.12798
4.0	0.23151	2.76778	0.1261
4.5	0.21277	2.46842	0.12299
5.0	0.19947	2.05296	0.10315
5.5	0.19045	2.02901	0.10838
6.0	0.18285	1.86219	0.09804
7.0	0.16834	1.60124	0.07734
8.0	0.17059	1.41272	0.06288
9.0	0.13886	1.25835	0.04607
10.0	0.13604	1.12835	0.02470
11.0	0.12868	0.95809	0.00348
12.0	0.14501	0.87954	-0.02130

Table S3. Fitted parameters of the Cole-Cole plots for complex **3** at H_{dc}= 0 G.

T / K	χ_S	χ_T	α
1.8	0.48094	8.43301	0.45611
3.0	0.33941	4.78538	0.42717
4.0	0.49971	3.48412	0.31414
4.5	0.27835	3.14935	0.36952
5.0	0.27868	2.67389	0.32779
5.5	0.28072	2.49665	0.30157
6.0	0.29217	2.17113	0.25876
7.0	0.27501	1.83756	0.20226
8.0	0.26229	1.65309	0.14499
9.0	0.24496	1.46295	0.10741
10.0	0.23002	1.31470	0.07824
11.0	0.20266	1.19410	0.06501
12.0	0.11540	1.09040	0.06598